diffusion-fundamentals.org

The Open-Access Journal for the Basic Principles of Diffusion Theory, Experiment and Application

Incorporating Internal Gradient and Restricted Diffusion Effects in Nuclear Magnetic Resonance Log Interpretation

Lilong Li,[1] *Songhua Chen,*[1]

[1] Baker Hughes Incorporated, Houston, TX, USA

Corresponding author: Lilong Li, Baker Hughes Incorporated, 2001 Rankin Road, Houston, TX 77073, E-Mail: lilong.li@bakerhughes.com

(received 13 September 2010, accepted 10 November 2010)

Abstract

It is shown that internal gradient combined with the restricted diffusion effect can significantly influence the D-T_2 cross plots, which are widely used for fluid typing in Nuclear Magnetic Resonance (NMR) well-logging applications. By using models that capture the most important features of the internal gradient in the sedimentary rocks, such effects can be accounted for in the D-T_2 inversion process, making fluid typing more accurate.

Keywords

NMR, well logging, internal gradient, restricted diffusion, porous media

1. Introduction

The problem of diffusive motion under pore-boundary constraints has many implications in a wide range of fields including biology, medicine, environmental science, and in the energy industry. NMR is an ideal candidate to study such a problem, but in a strong magnetic field, the internal gradient created due to magnetic susceptibility contrast becomes a very important issue. In the case of sedimentary rocks, even a weak magnetic field can generate a strong internal gradient that obscures the gradient from the external field. Practically, however, it is difficult to track down these effects due to the complexity of the natural pore space and paramagnetic materials distribution.

In this paper we demonstrate that the complexity of natural pore space and the variation in the distribution of paramagnetic materials can be simplified, depending on the situation. One issue of particular interest is the D-T_2 cross plot for fluid typing, which is used widely in well-logging applications in the oil industry. It is easily postulated that the internal gradient effect will cause an overestimate of diffusivity. Modern logging tools employ multiple frequencies and associated gradients, and numerous sets of acquisition parameters. Consequently, the exact influence of the internal gradient with the restricted diffusion effect is unknown. A free diffusion equation that disregards the internal gradient is still used exclusively for data interpretation. We demonstrate that simple internal gradient models can account for most

salient factors of internal gradient in sedimentary rocks and result in more accurate fluid typing in NMR well logging.

2. Methods

2.1 Theory

The guiding equation for magnetization evolution under a field gradient is:

$$\left(\frac{\partial}{\partial t} - D\nabla^2 + i\gamma \boldsymbol{g}\cdot\boldsymbol{r}\right)m(\boldsymbol{r},t) = 0 \tag{1}$$

where ∇^2 is the Laplace operator, D is the diffusion coefficient, γ is the gyromagnetic ratio, and m is the magnetic moment. This equation was proposed by Torrey [1] by modifying the Bloch equation to account for the diffusive motion. Under geometrical confinement, the proper boundary condition is:

$$D\frac{\partial}{\partial n}m(\boldsymbol{r},t) + \rho m(\boldsymbol{r},t) = 0 \tag{2}$$

where $\partial/\partial n$ is the outward normal derivative, and ρ is the surface relaxivity.

Eq. (1) can be solved by the finite difference method [2] or the multiple correlation function (MCF) approach developed by Grebenkov [3]. Alternatively, the Monte Carlo technique can be used to simulate the Brownian motion of individual spins [4].

2.2. Models of the internal field

When diffusion is restricted between parallel planes (1D slab), we used the following model for the internal field:

$$B_z^l = \delta\chi B_0 \sin(\frac{\pi r}{L}) \quad 0 \le r \le L \tag{3}$$

where L is the length between the two parallel planes.

In the case of spherical boundaries (3D sphere), the following internal field distribution along z direction was used:

$$B_z^s = \delta\chi B_0 \cos(\frac{\pi r}{2R})\cdot\cos(\theta) \quad 0 \le r \le R, 0 \le \theta \le \pi \tag{4}$$

We chose these two models based on the criteria that the maximum of the internal field is proportional to $\delta\chi B_0$, the field gradient is normally higher at the liquid-solid interface, and the profile of the internal field does not change with the size of the grains.

2.3. Numerical methods

The finite difference method follows the Crank-Nicolson procedure, as described in Ref. [5]. The MCT approach is explained in detail in Ref. [3].

2.4. Random Walk Simulation

We used a random pack of 10,000 equal spheres to represent the internal field contribution to a single pore in the middle of the grain pack. The magnetic field was calculated by summing up the contribution from each of the grain. To avoid such a large summation at each step of the random walk, we chose to do a simulation on a discrete 100x100x100 grid, as was done in Ref. [4].

3. Results and Discussions

3.1. Effects of the Internal Gradient and Restricted Diffusion

To investigate whether internal gradients effects have a significant impact on T_2-Diffusion inversion in fluid typing applications, we produced synthetic data using the 3D sphere internal field model described in the previous sections, with acquisition parameters used in the field. Fig. 1 shows the inversion result of such synthetic data with the original method. Every block in Fig. 1 represents the inversion result of the case corresponding to the respective pore size and magnetic susceptibility contrast. The surface relaxivity ρ was set as 10 μm/s, and the relationship between pore size and surface relaxation is assumed to be:

$$T_{2S} = \rho \frac{S}{V} \tag{5}$$

Note that 1D inversion results were also produced, with both the MCF method and the finite difference method. Both methods produce results that look similar to Fig. 1, so they are not duplicated here.

From Fig. 1, it is obvious that the internal gradient has a substantial influence on fluid-typing measurements, especially when the magnetic susceptibility contrast is high (not uncommon in the case of sedimentary rocks where a significant amount of paramagnetic materials may be present). With the surface relaxivity parameter set to 10 μm/s, the maximum internal gradient effect corresponds to the pore size of 5-10 μm. For smaller and larger pores, the motional averaging and slow diffusion regimes are approached respectively and the internal gradient effects are much weaker. In the case where the internal gradient does not exist ($\delta\chi$=0), as pore sizes become smaller, the diffusivity that comes from inversion deviates further from the input number, suggesting ever stronger effects from restricted diffusion.

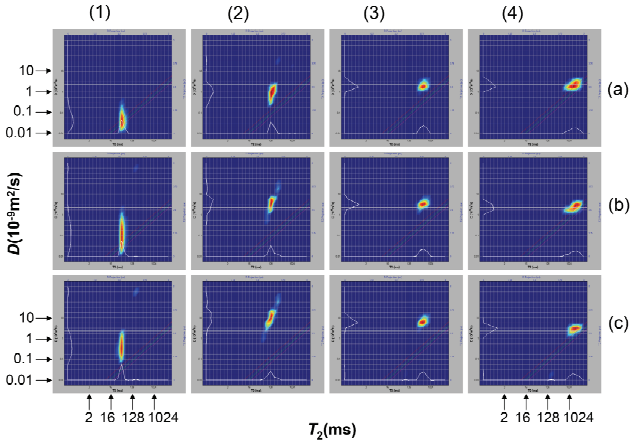

Fig. 1: Inversion results using the original method, with synthetic data that takes into account the internal gradient and restricted diffusion effects. In the row direction: (a) $\delta\chi$=0, (b) $\delta\chi$=0.0001, (c) $\delta\chi$ =0.0002. In the column direction: (1) r=1μm, (2) r=3μm, (3) r=10μm, (4) r=30μm. Here $\delta\chi$ is the magnetic susceptibility contrast, and r is the representative pore size.

3.2. Improved Inversion of Synthetic Data

With free diffusion, the rate of relaxation is determined by:

$$\frac{1}{T_2} = \frac{1}{T_{2S}} + \frac{1}{12} D(\gamma g \cdot TE)^2 \tag{6}$$

where $1/T_{2S}$ is the rate of relaxation due to contact with the solid surface. With restricted diffusion and a complex distribution of the internal gradient, such an analytical formula does not exist. Fortunately, for the inversion problem a numerical solution still exists due to the discrete nature of the inversion algorithm. In this case, we can write the rate of relaxation as a function of various variables:

$$R_{i,j,k,l,m,n} = R(D_i, T_{2j}, \rho_k, r_{(j,k)}, \delta\chi_l, B_m, g_m, TE_n) \tag{7}$$

where B_m, g_m are the magnetic field and its gradient generated by the tool, TE_n represents one instance of TE as configured in the pulse sequence, ρ_k and $\delta\chi_l$ are possible numbers for surface relaxivity and magnetic susceptibility contrast, respectively, and D_i and T_{2j} represent one point in the 2D inversion grid. As all variables take discrete numbers, the possible values of R become a huge matrix. This matrix is still manageable and can be numerically computed ahead of time and stored. During the process of inversion, the values can be fetched with minimal delay.

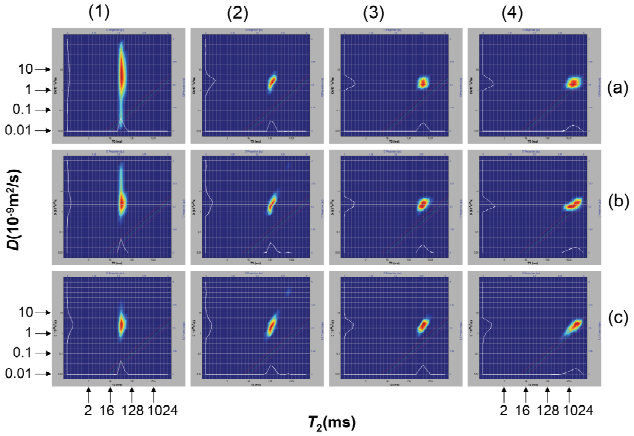

Fig. 2: Inversion results using improved method, with the same input data and plotting parameters as in Fig. 1.

With this discretization in mind, we substituted the real-time calculation according to Eq. (6) with fetched data according to Eq. (7) in the inversion process. The result is shown in Fig. 2. From Fig. 2, we see that for the synthetic data, the inversion result was a significant improvement over the original method. The remaining difference between the inversion results and the original input data (in terms of T_2 and D) is most probably due to discretization.

3.3. A Model to Represent the Statistical Profile of the Internal Field

To apply our method to real data, a suitable model for internal field distribution has to be developed. In principle, a pore-scale model of sedimentary rock can be used to calculate the matrix in Eq. (7). This calculation, though, requires a large amount of time. To save time, it is better to develop a simplified model for calculating the matrix. We decided to verify whether a simplified model such as the one described by Eq. (4) can be used to statistically represent the internal field in a rock.

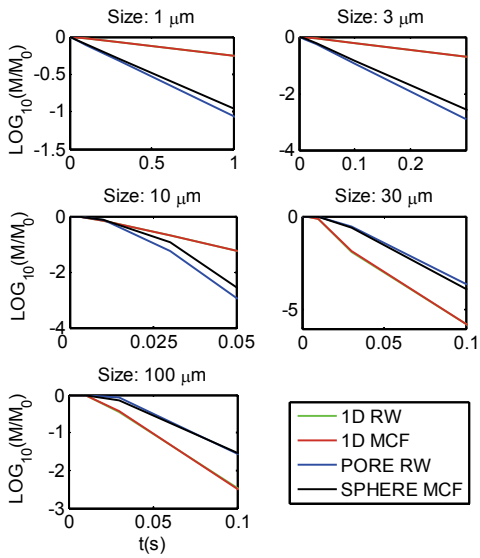

Fig. 3: T_2 relaxation comparison with confinement under different sizes of pores. 1D RW means random walk calculation using a 1D slab model, and 1D MCF means Multiple Correlation Function calculations using a 1D model. Likewise, PORE RW means random walk calculations in a real pore model, and SPHERE MCF means Multiple Correlation Function calculation using a 3D sphere model. 1D RW and 1D MCF lines overlap in the figure.

We used a random walk of a single pore in the middle of a sphere pack to calculate the T_2 decay and compared that with the MCF calculation from the simple model previously described. Fig. 3 shows the comparison. 1D random walk was also performed with the same field distribution in the MCF calculation to test the accuracy of the random walk calculations. As shown in Fig. 3, the red and the green data points look identical which suggests that the random walk procedure is reliable. We can see a difference between the 3D simple model calculation with MCF and the 3D random work results in a single pore, but the difference is not that significant in terms of real applications. Furthermore, we believe that the profiles of the internal gradient in different pores are similar statistically, as was demonstrated by others [6]. Thus, we conclude that the 3D simple model, instead of a complex pore-scale model, may be used for the inversion process.

3.4. Verification with logging data

Fig. 4 demonstrates the inversion results of field logging data at a certain depth. It can be easily seen that because our physical model is closer to reality than previous assumptions, the inversion results are much more reasonable as the water signal appears on the water diffusivity line and the separation of the gas signal and that of water becomes clearer. We believe the new method gives more presentable and more accurate results.

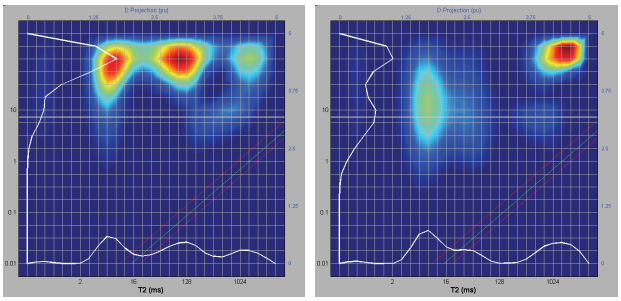

Fig. 4: Inversion results using logging data, left, with the original method; right, with the new method.

4. Conclusions

We have proposed an approach where a simple model for pore and internal gradient distribution can be used. The model may not perfectly represent the real pore system in a rock, but it captures the most important features of the internal gradient and can statistically represent the internal field distribution. By taking advantage of the discrete nature of the inversion algorithm, MCF calculations can generate the set of matrixes that will be used in the inversion process, thus avoiding the need for analytical solutions. By incorporating the internal gradient effect this way in the inversion process, we demonstrated that drastic improvements can be achieved compared to the traditional free diffusion interpretation method when the internal gradient effect is significant. It should be noted though that the possible internal gradients models are not confined to the one used in this paper. Other internal field distribution models will be explored in the future. In principle, even a complicated rock model can be used if the computation time using Monte Carlo simulations is not a major concern.

References

[1] H.C. Torrey, Phys. Rev., 104 (1956) 563–565.
[2] P.N. Sen, A. Andre, S. Axelrod, J. Chem. Phys., 111 (1999) 6548-6555
[3] D.S. Grebenkov, Rev. Mod. Phys, 79 (2007) 1077-1137
[4] R.M.E. Valckenborg, H.P. Huinink, J.J.v.d. Sande, K, Kopinga, Phys. Rev. E., 65 (2002) 021306
[5] M.H. Blees, J. Mag. Res., Ser. A, 109 (1994) 203-209
[6] Y.Q. Song, Con. Mag. Res. A, 18A (2003) 97-110